Radar-based Dataset Development for Human Activity Recognition

A. Ahmed and Y. D. Zhang

Advanced Signal Processing Laboratory, Temple University, Philadelphia, Pennsylvania, USA
{ammar.ahmed, ydzhang}@temple.edu

Human activity recognition (HAR) is an important research problem and considerable efforts have been made in the past two decades to develop successful solutions. Datasets developed for HAR serve as a baseline for evaluating new HAR algorithms and play a pivotal role in advancing the research efforts in this domain. Hundreds of datasets have been developed by various researchers which focus on different types of motions and activities [1]. In this context, most of the efforts have been invested in developing the datasets which contain either the video or clips of 2D images of different types of motions. Due to the advent of 3D sensors, modern datasets also contain the information of the motion as well as the depth [2].

There are several intrinsic challenges associated with image- or video-based HAR. The HAR strategies developed based on visual datasets cannot work for challenging visibility conditions or in the absence of light. There are also privacy concerns associated with image- and video-based HAR.

These facts have motivated great interest to develop radar-based HAR methods [3]. Such efforts are still in an early phase and generally exploit Doppler and micro-Doppler analysis of radar signals reflected by the human body. The basic idea is that different human activities exhibit unique Doppler and micro-Doppler signatures which can be classified by using their time-frequency characteristics. Recently, cost-effective millimeter-wave radar systems with high Doppler sensitivity enabled easier access to detecting and classifying human activities. Since the received micro-Doppler signals do not provide facial and other sensitive privacy information, radar-based HAR is much more easily accepted without privacy-related concerns.

In this abstract, we present a radar-based dataset for human activity recognition (Rad-HAR) that exploits continuous-wave (CW) radar signals. The dataset is collected for scenarios where one human subject makes different motions in front of the radar. For this purpose, we use the Ancortek SDR-KIT-2500 [4] software-defined transmitter-receiver system which consists of one transmitter and one receiver as shown in Figure 1. CW signals with carrier frequency of 25 GHz are used for the dataset development. We provide the raw as well as processed micro-Doppler signals in the DAT format which can be imported in several popular programming languages. Several MATLAB examples are provided to perform data processing exploiting time-frequency analysis techniques.

Figure 1. Ancortek SDR-KIT-2500 module [4].

Signal Model: Consider a human body as the collection of P point targets, which are located in the front of the radar. The transmit radar signal is given by:

$$s(t) = A \exp(\mathrm{j}2\pi f_c t), \tag{1}$$

where A is the transmit signal amplitude, f_c is the carrier frequency, and t is the fast time. The instantaneous range of the pth point target with respect to the radar is:

$$R_p(t) = R_{0,p} + \int_{t_0}^{t} v_p(u) \cos(\varphi_p(u))\, \mathrm{d}u, \tag{2}$$

where t_0 is the start time, $R_{0,p}$ is the initial range of the pth point target, whereas $v_p(t)$ and $\varphi_p(t)$ respectively denote the velocity and angle of the pth target at time instant t with respect to the radar.

Subsequently, the signal reflected by pth point target is expressed as:

$$r_p(t) = A_p(t)\exp\left(\mathrm{j}2\pi f_c(t-\tau_p)\right) = A_p(t)\exp\left(\mathrm{j}2\pi f_c\left(t-\frac{2R_p(t)}{c}\right)\right), \tag{3}$$

where $A_p(t)$ is the amplitude of the target echo at time t which depends on the transmit signal amplitude A, the range $R_p(t)$, and the radar cross-section of the point target. Moreover, $\tau_p = 2R_p(t)/c$ is the time delay due to the round-trip range of the pth point target, and c is the electromagnetic propagation speed.

Using Eq. (3) and the known carrier frequency f_c, we can extract the baseband signal received corresponding to the pth point target as:

$$\bar{r}_p(t) = r_p(t)A_c\exp(-\mathrm{j}2\pi f_c t) = B_p(t)\exp\left(-\mathrm{j}4\pi f_c\frac{R_p(t)}{c}\right), \tag{4}$$

where A_c is the amplitude of the demodulating carrier waveform and $B_p(t)$ is the baseband amplitude of the resulting received signal. The time-varying Doppler frequency corresponding to the pth point target is expressed as:

$$f_{D,p}(t) = -\frac{2v_p(t)\cos\varphi_p(t)}{c}f_c = -2\frac{f_c}{c}\frac{d}{dt}R_p(t). \tag{5}$$

Since the human body is the collection of all point targets contained in the set P, the overall baseband signal corresponding to the entire human body is represented by the collection of signals from all these point targets, given by:

$$\bar{r}(t) = \int_{p\in P}\bar{r}_p(t)\mathrm{d}p = \int_{p\in P}B_p(t)\exp\left(-\mathrm{j}4\pi f_c\frac{R_p(t)}{c}\right)\mathrm{d}p. \tag{6}$$

The velocities of different body parts generally differ from each other. In this context, time-frequency analysis is suitable to characterize the resulting Doppler and micro-Doppler signatures. In this abstract, spectrogram generated from the short-time Fourier transform is adopted, expressed as:

$$S_{\bar{r}}(t,f) = \left|\int_{-\infty}^{\infty}\bar{r}(t)h(t-k)e^{-\mathrm{j}2\pi fk}dk\right|^2, \tag{7}$$

where $h(t)$ is a suitable window function.

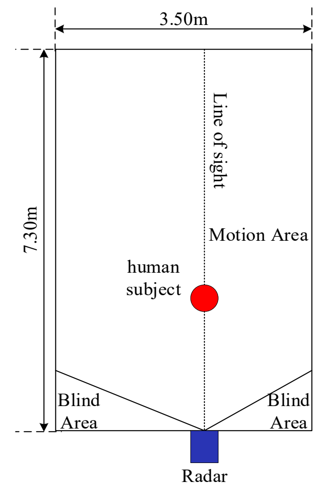

Figure 2. The lab environment in which the Rad-HAR dataset is acquired.

Dataset: The Rad-HAR dataset was acquired at the Advanced Signal Processing Laboratory (ASP Lab) of Temple University. The data collection was approved by the Institutional Review Board (IRB) of Temple University. The layout of the laboratory is given in Figure 2. The dataset consists of six different types of human movements as shown in Table 1. Data due to the human motions are recorded at different sampling rates and stored as raw data in the DAT file format. The data for each type of motion are placed in separate folders with folder name acting as the data label. These files contain raw in-phase and quadrature (I/Q) data in the form of complex sinusoids expressed in Eq. (6).

The Rad-HAR dataset also contains processed data. For such processed data, the direct-

Table 1. The Rad-HAR Dataset

	Type of motions	Raw data length (sec)	Raw data sample rate (ksample/sec)	Number of three-second data segments
Facing towards the radar	Boxing	60/30	512	196
	Clapping	15/180	128/512	199
	Hand waving	60/30/15	512/512/128	199
	Piaffe / Mark time	15/300	128/512	199
	Running towards radar	3/6	128/128	50
	Walking towards radar	3/6	512/128	100
Facing opposite to the radar	Walking away from radar	6	128	50
	Running away from radar	6	128	97

current (DC) offset is removed because it mainly represents strong clutter near 0 Hz in the Doppler domain and obscures target motion recognition. Furthermore, we clip the data of each class into three-second segments which can be readily employed to observe the Doppler signatures in the time-frequency domain. We downsampled all the processed data to 64 ksample/sec which is high enough to capture the desired human motions.

Instruction to accessing the Rad-HAR dataset is provided at [5] under the “Resources” section.

Examples: As an example to accessing the Rad-HAR dataset, we present the time-frequency characteristics of selected received radar signals. The spectrogram computed for the first three second of the data in each class is shown in Figure 3. It is evident that each class has unique Doppler and micro-Doppler signatures for them to be separately recognized. For motions that generate noticeable changes in the range between the target and the radar, such as walking and running, the spectrogram clearly reflects that the propagation loss of the radar signals increases with the range. An example of the HAR performance on the Rad-HAR dataset by exploiting deep learning approaches can be found in [6].

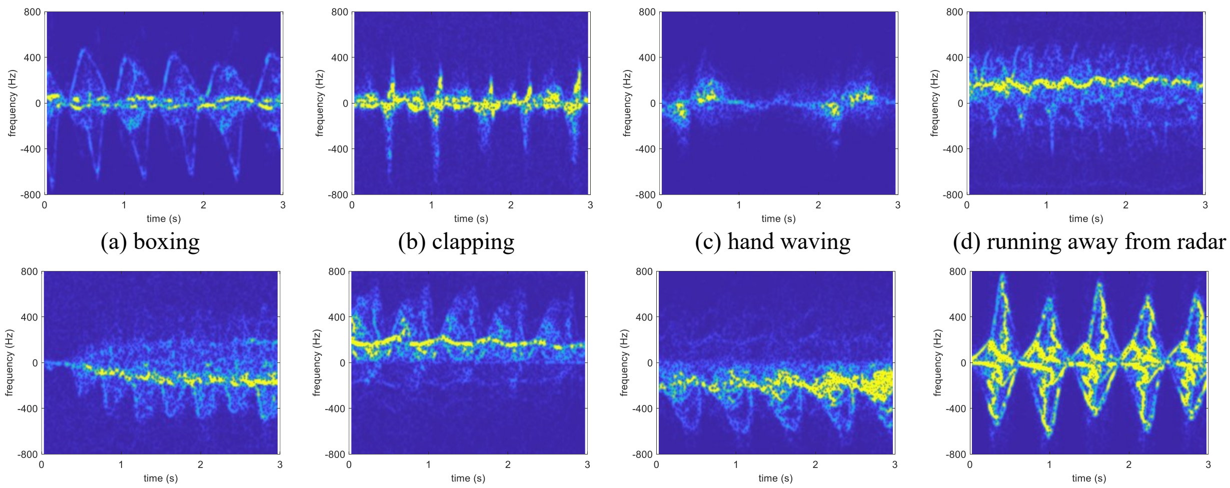

(a) boxing (b) clapping (c) hand waving (d) running away from radar

(e) running towards radar (f) walking away from radar (g) walking towards radar (h) mark time

Figure 3. Spectrogram of different types of motions with respect to radar in Rad-HAR dataset

ACKNOWLEDGEMENT

We acknowledge the members of the Temple University ASP Lab who participated in the data collection.

REFERENCES

[1] R. Singh, A. Sonawane, and R. Srivastava, “Recent evolution of modern datasets for human activity recognition: A deep survey,” *Multimedia Systems*, vol. 26, no. 1, pp. 83–106, 2020.

[2] J. Zhang, W. Li, P. O. Ogunbona, P. Wang, and C. Tang, “RGB-D-based action recognition datasets: A survey,” *Pattern Recognition*, vol. 60, pp. 86–105, Dec. 2016.

[3] M. G. Amin, Y. D. Zhang, F. Ahmad, and K. C. Ho, “Radar signal processing for elderly fall detection,” *IEEE Signal Processing Magazine*, vol. 33, no. 2, pp. 71-80, March 2016.

[4] “SDR-KIT 2500B,” *Ancortek Inc.*, 2019. [Online]. Available: *https://ancortek.com/sdr-kit-2500b/*.

[5] “Radar-based Human Activity Recognition (Rad-HAR) Dataset,” *Temple University Advanced Signal Processing Laboratory*, 2018. [Online]. Available: *http://asplab.net/*.

[6] M. Wang, Y. D. Zhang, and G. Cui, “Human motion recognition exploiting radar with stacked recurrent neural network,” *Digital Signal Processing*, vol. 87, pp. 125-131, April 2019.